52nd IEEE Conference on Decision and Control
December 10-13, 2013. Florence, Italy

Dynamics-aware Optimal Power Flow

Enrique Mallada and Ao Tang

Abstract— **The development of open electricity markets has led to a decoupling between the market clearing procedure that defines the power dispatch and the security analysis that enforces predefined stability margins. This gap results in market inefficiencies introduced by corrections to the market solution to accommodate stability requirements. In this paper we present an optimal power flow formulation that aims to close this gap. First, we show that the pseudospectral abscissa can be used as a unifying stability measure to characterize both poorly damped oscillations and voltage stability margins. This leads to two novel optimization problems that can find operation points which minimize oscillations or maximize voltage stability margins, and make apparent the implicit tradeoff between these two stability requirements. Finally, we combine these optimization problems to generate a dynamics-aware optimal power flow formulation that provides voltage as well as small signal stability guarantees.**

I. Introduction

The optimal power flow (OPF) is the optimization problem used for finding the best power scheduling of a network that minimizes an objective function (e.g. market welfare, losses, generation cost and voltage magnitudes) subject to physical and operational constraints. It has a long history in the power systems community dating back to at least 1962 with the seminal work of Carpentier [1]. It has since become a fundamental tool for defining prices and arbitrating electricity markets, and many different algorithms have been proposed to solve OPF [2], [3].

On the other hand, stability of the power network has been one of the major concerns of every utility company. When a blackout occurs, the resulting economic impact can cost between several hundred million dollars and a few billion dollars [4]. Thus, utility operators are constantly monitoring the network state in order to avoid different types of instabilities that a power system might experience. These include, for instance, voltage collapse/instability [5], small signal oscillations/instability [6] and transient instability [7].

Different methods have been developed to assess and prevent each individual stability problem. Voltage stability, for example, can be analyzed using screening and ranking methods [8] and continuation methods that investigate the available transfer capability of the current operating point [9]. Small signal oscillations, on the other hand, are locally damped using Power System Stabilizers (PSS) in the exciter control loop [6] and globally damped using either power electronics, such as Flexible AC Transmission System (FACTS) devices [10], or using Phasor Measurement Unit (PMU) information in the PSS loop [11]. Finally, transient stability is analyzed using time domain integration [12] or the controlling unstable equilibrium point methodology [13].

Even though these methods have diverse objectives and therefore employ different techniques, they all require as input an initial operating point, which is usually obtained by solving certain OPF problem. While this may not be a big issue for transient stability as it also depends on the specific fault in consideration, the procedure used to clear it, and the time needed to recover from it (fault clearing time) [14], it is certainly critical in voltage stability and small signal oscillation studies because the voltage collapse margin and stability of the operating point are directly influenced by the scheduling choice (solution of OPF).

Therefore, without any additional considerations the scheduling obtained by the OPF may produce fragile or even unstable solutions. This is prevented nowadays in many utility companies by performing a day ahead detailed stability analysis based on historic records and predictions which is translated into line flow constraints. However, these additional constraints does not have a clear dynamical meaning that can be used to indicate how robust is the current solution and in some scenarios are not enough. It is common to introduce corrections on the scheduling online to prevent instabilities which can generate market inefficiencies.

In other words, the existing methodology is unable to contemplate the fact that these two problems are intrinsically coupled. This problem has been identified and studied over the last 15 years and several methods have been proposed to include voltage stability constraints in the OPF problem [16], [17]. However, adding small signal stability constraints has been a daunting task because it usually requires constraining or computing sensitivity of several (if not all) eigenvalues of the system [15]. Furthermore, these procedures can sometimes produce undesired outcomes since there is a tradeoff between asymptotic rate of convergence ($\max \Re[\lambda_i]$) and transient amplitude.

In this paper we overcome this problem by using a novel performance metric known as pseudospectral abscissa that can balance transient amplitude and asymptotic convergence rate [18]. Using this metric, we propose an optimization framework that not only imposes voltage and small signal stability constraints on the OPF without explicitly computing and constraining the eigenvalues of the system, but also finds the performance limits of the system.

The rest of this paper is organized as follows. In Section II we describe the dynamics of a power network, the different stability issues it can experience and the OPF problem. We then bring in the pseudospectral abscissa in Section III and

Department of Electrical and Computer Engineering, Cornell University, Ithaca, NY 14853. Emails: {em464@,atang@ece.} cornell.edu. Research supported in part by National Science Foundation Grant CCF-0835706 and in part by Office of Naval Research Grant N00014-11-1-0131.

show how it can be used to measure and optimize voltage stability margins, oscillations and robustness. This naturally leads to our Dynamics-aware OPF formulation. We illustrate several properties of our new optimization framework using two different test cases, including the widely used IEEE 39-bus New England power grid test case in Section IV. We conclude in Section V.

II. Background

We now proceed to describe two models commonly used in the study of OPF and power systems dynamics: *static* and *dynamic* models. Each has its specific use and the level of detail depends on the problem in consideration.

A. Static Power Network Modeling

The *static* model of a power network defines the physical relationship that the state at each bus must satisfy for the system to be at equilibrium. In this model, the state is solely represented by the complex voltage $V_k = |V_k|e^{i\theta_k}$ at each bus $k \in \mathcal{N}$, which in order to be at equilibrium, must satisfy the flow conservation equations, also known as *power flow equations*. These equations basically state that the surplus (or deficit) in generation at a given bus should match the outgoing (incoming) power flow to (from) the neighboring buses and ground, i.e.

$$|V_k|^2 y_{kk}^* + \sum_{l \sim k} S_{kl} = P_{G_k} + iQ_{G_k} - (P_{D_k} + iQ_{D_k}). \quad (1)$$

Here, $P_{G_k} + iQ_{G_k}$ is the complex power generated, $P_{D_k} + iQ_{D_k}$ is the complex power demanded at bus k, $S_{kl} = P_{kl} + iQ_{kl} := V_k(V_k - V_l)^* y_{kl}^*$ is the complex line flow from k to l, y_{kk} is the bus shunt admittance and y_{kl} is the line admittance. Loads are usually modeled as constant impedance (Z), constant current (I) or constant power (P). When the loads are modeled by constant impedance or constant current models, P_{D_k} and Q_{D_k} are functions of the voltage magnitude at the bus. A well-accepted model for static loads is the ZIP model which is a convex combination of the three, i.e.

$$P_{D_k} = P_{0,k}\left(a_{1,k}\left(\frac{|V_k|}{V_{0,k}}\right)^2 + a_{2,k}\left(\frac{|V_k|}{V_{0,k}}\right) + a_{3,k}\right) \quad (2a)$$

$$Q_{D_k} = Q_{0,k}\left(b_{1,k}\left(\frac{|V_k|}{V_{0,k}}\right)^2 + b_{2,k}\left(\frac{|V_k|}{V_{0,k}}\right) + b_{3,k}\right) \quad (2b)$$

Since this model is sufficient to characterize the static properties of the network, such as the existence of a stationary solution of the power flow equations (1), voltage magnitudes $|V_k|$, line flows P_{kl} and S_{kl}, and losses $P_{kl}+P_{lk}$, it is used for the computation of optimal power flow and the study of voltage stability.

To simplify notation, we will use from now on $x_s := ((|V|), (\theta))^T$ as the vector of the static network states, $u_s := ((P_G), (Q_G))^T$ as the vector of static control variables and $v_s := ((P_0), (a_1), (a_2), (a_3), (Q_0), (b_1), (b_2), (b_3))^T$ as the vector of load parameters. Thus, the power flow equations (1) can be compactly defined as $F(x_s, u_s, v_s) = 0$.

1) Optimal Power Flow: Let $f_k(V_k, P_{G_k}, Q_{G_k})$ denote the cost function associated with bus k. In most cases, f_k depends solely on P_{G_k} but it can be extended to more general scenarios. Then, the optimal power flow can be formulated as

$$\mathbf{OPF}: \underset{x_s, u_s}{\text{minimize}} \quad c(V, P_G, Q_G) := \sum_{k \in \mathcal{N}} f_k(V_k, P_{G_k}, Q_{G_k}) \quad (3)$$

subject to

$$F(x_s, u_s, v_s) = 0 \quad (4a)$$

$$P_k^{\min} \le P_{G_k} \le P_k^{\max}, \qquad \forall k \in \mathcal{N} \quad (4b)$$

$$Q_k^{\min} \le Q_{G_k} \le Q_k^{\max}, \qquad \forall k \in \mathcal{N} \quad (4c)$$

$$V_k^{\min} \le |V_k| \le V_k^{\max}, \qquad \forall k \in \mathcal{N} \quad (4d)$$

$$P_{kl} \le P_{kl}^{\max}, \qquad \forall (k,l) \in \mathcal{L} \quad (4e)$$

$$|S_{kl}| \le S_{kl}^{\max}, \qquad \forall (k,l) \in \mathcal{L} \quad (4f)$$

The list of methods to solve this problem is vast. Some of the most commonly used are primal dual interior point method [2] and newton method [19].

2) Voltage Stability: Voltage stability refers to the ability of the system to preserve voltage magnitudes within its nominal values and avoid voltage collapse. A voltage collapse occurs when changes on u_s or v_s make two solutions of (4a) coalesce and disappear in a **Saddle Node Bifurcation**. This is evidenced by the presence of a real eigenvalue of the Jacobian matrix

$$J(x_s, u_s, v_s) = D_{x_s} F(x_s, u_s, v_s) \quad (5)$$

on the imaginary axis.

It is important to notice that the OPF problem (3)-(4) guarantees voltage stability since its solution satisfies the power flow constraints (4a). However, the stability margins may not be large and a small fluctuation on the demand can thus produce a voltage collapse.

This has motivated the development of optimization-based techniques that define some distance measure, compute the smallest distance to voltage collapse (e.g. [20]) and improve it [21]. These developments have led to a solid integration of voltage stability measures as constraints or as part of the objective function of the OPF problem [16], [17]. Yet, none of them considers the effect of the outcome of these solutions on the dynamics of the power system.

B. Dynamic Power Network Modeling

The dynamics of a power network is represented by a set of differential algebraic equations (DAEs) [22]

$$\dot{x} = f(x, z, u, v) \quad (6)$$

$$0 = g(x, z, u, v). \quad (7)$$

where x and z are the slow and fast state variables respectively, u are the control inputs, such as power generation, active voltage regulators (AVR) set points, transformers taps, etc., and v are the exogenous parameters such as power demand. Equation (6) represents the dynamics of the system devices including generators, power electronics and controllers, and

(7) are the algebraic equations of the generators stators, power electronics and network power flows.

Equations (6)-(7) form a more detailed model than the static model (1)-(2) and include in (x, z), u and v, the values of x_s, u_s and v_s, respectively. In fact, equation (4a) is a subset of (6)-(7).

Remark 1: It is important to notice that when x_s, u_s and v_s satisfy $F(x_s, u_s, v_s) = 0$, we can find x, z such that $f(x, z, u, v) = 0$ and $g(x, z, u, v) = 0$. In fact, given x_s, u_s and v_s there is a unique x, z whose phase and voltage magnitude values are equal to x_s. This will be used in later sections to formulate our dynamics-aware OPF. Overall, the level of detail in the dynamic model is essential when one wants to study dynamic phenomena such as small signal oscillations.

1) Small Signal Oscillations: Small signal oscillations are the effect of a **Hopf Bifurcation** in which a stable equilibrium point becomes unstable and a limit cycle appears, or the effect of poorly damped modes of stable operating points. These oscillations can be studied by linearizing the system (6)-(7) around an equilibrium point (x^*, z^*, u^*, v)

$$\dot{x} = [D_x f]x + [D_z f]z + [D_u f]u \tag{8a}$$

$$0 = [D_x g]x + [D_z g]z + [D_u g]u \tag{8b}$$

and assuming that $D_z g(x^*, z^*, u^*, v)$ is nonsingular[1] to obtain reduced system

$$\dot{x} = Ax + Bu \tag{9}$$

$$\text{where} \quad A = D_x f - D_z f \left(D_z g\right)^{-1} D_x g \tag{10}$$

$$\text{and} \quad B = D_u f - D_z f \left(D_z g\right)^{-1} D_u g.$$

The presence of small signal oscillations is evidenced by a complex conjugate pair of eigenvalues of A close to the imaginary axis. As previously mentioned, small signal stability can usually be improved by designing controllers (e.g. PSS and FACTS) such that in closed loop A has eigenvalues with smaller damping ratios [6], [11]. However, none of these solutions considers the fact that (10) depends on the solution of the power scheduling (encoded in u^*) and that oscillations can appear if the market solution moves the system towards a more stressed condition. This generates the need for re-dispatching procedures that correct the scheduling in order to avoid small signal instabilities.

The current way of dealing with the above issue is by either iteratively adding constraints to successive OPF instances based on eigenvalues sensitivity information [15] or solving an OPF instance using an interior point method with a constraint on the real part $\Re[\lambda_i]$ of every critical eigenvalue [23]. Besides the computational complexity of these methods (one of them has to solve several OPFs and the others compute second order sensitivity of eigenvalues), it is also important to notice that most of them essentially use $\max \Re[\lambda_i]$ as a stability constraint to avoid Hopf Bifurcations, and disregard any other performance or robustness metric in the optimization. The only exception is [15] which successively adds approximate damping ratio constraints to each OPF instance solved. Unfortunately neither solution provides a satisfactory answer. On the one hand, using $\max \Re[\lambda_i]$ may produce undesired effects because, as one gets closer to a local minimum of the function the system can exhibit large amplitude transients [18]. On the other hand, adding damping constraints on the eigenvalues has no effect on voltage stability, as a real eigenvalue can be arbitrarily close to the imaginary axis without meeting any damping ratio constraint. This difficulty directly motivates us to formulate a dynamics-aware OPF in the next section.

[1]The nonsingularity of $D_z g(x^*, z^*, u^*, v)$ is a standard assumption in power system stability studies that is generally satisfied in the presence of a slack bus.

III. Dynamics-aware Optimal Power Flow

In this section we show that the use of pseudospectral abscissa $\alpha_\varepsilon(A)$ provides a convenient framework that not only balances transient amplitude and asymptotic convergence rate, but also jointly guarantees voltage and small signal stability. This subsequently leads to a new optimization formulation that can jointly enforce both stability constraints with a single performance metric.

Given $\varepsilon \geq 0$ the pseudospectrum Λ_ε of a matrix A is defined as the set of eigenvalues of all matrices $X \in \mathbb{C}^{n\times n}$ satisfying $||X - A||_2 \leq \varepsilon$ where $||\cdot||_2$ is the spectral norm. With this notation, the pseudospectral abscissa is defined by

$$\alpha_\varepsilon(A) = \max\{\Re[z] : z \in \Lambda_\varepsilon(A)\}.$$

When $\varepsilon = 0$, $\alpha_0(A)$ reduces to the spectral abscissa which is equivalent to the constraint in [23]. There are several advantages on using pseudospectral abscissa instead, which we now summarize:

- Unlike $\alpha_0(A)$, $\alpha_\varepsilon(A)$ is locally Lipschitz with respect to A and thus easier to numerically compute.
- Let $\beta(A)$ be the shortest distance between A and an unstable matrix $X \in \mathbb{C}^{n\times n}$, then the following relationship follows:

$$\alpha_\varepsilon(A) \leq 0 \iff \beta(A) \geq \varepsilon \iff \mathcal{H}_\infty(A) \leq \frac{1}{\varepsilon}$$

  Here, $\mathcal{H}_\infty(A)$ is the $\mathcal{H}_\infty$ norm of the system [24], i.e. $\mathcal{H}_\infty(A) = \sup_{\omega\in\mathbb{R}} \sigma_{\max}(H(j\omega))$, where $\sigma_{\max}(H(s))$ is the maximum singular value of the transfer function $H(s) = (A - sI)^{-1}$.
- $\alpha_\varepsilon(A)$ captures several dynamic properties for different values of ε. For $\varepsilon = 0$, $\alpha_\varepsilon(A)$ is the asymptotic rate. If $\alpha_\varepsilon(A) = 0$ then $\varepsilon^{-1} = \mathcal{H}_\infty(A)$ and when $\varepsilon \to +\infty$, $(\alpha_\varepsilon(A) - \varepsilon)$ is the initial rate of decay.

We refer the reader to [25] for proofs of these claims.

With these nice properties, we now propose the following optimization problems to study the performance limits of a power network.

$$\mathbf{H}_\infty : \underset{\varepsilon\geq 0, x, z, u}{\text{minimize}} \quad h(\varepsilon)$$

$$\text{subject to} \quad (4) \tag{11a}$$

$$\alpha_\varepsilon(A(x, z, u, v)) \leq 0 \tag{11b}$$

Remark 1 guarantees that by satisfying (4a) we can find (x, z, u, v) that satisfies the equilibrium equations of (6)-(7) and therefore we do not need (6)-(7) as constraints.

The function $h(\varepsilon)$ is decreasing, which guarantees that the optimal solution $(\varepsilon^*, x^*, z^*, u^*)$ of $\mathbf{H}_\infty$ has the constraint (11b) met with equality and makes $\frac{1}{\varepsilon^*} = \mathcal{H}_\infty(A(x^*, z^*, u^*, v))$. Thus, this problem finds the optimal configuration in terms of $\mathcal{H}_\infty(A(x, z, u, v))$. Furthermore, the solution of $\mathbf{H}_\infty$ also guarantees voltage stability, since (6)-(7) has a stable equilibrium, and ensures a robust stability radius of ε^*. In this paper we will use $h(\varepsilon) = -20\log_{10}(\varepsilon)$, which amounts to the maximum power gain in decibels (dB) of the transfer function $H(s)$ when $\alpha_\varepsilon(A(x, z, u, v)) = 0$.

Alternatively, one could choose to sacrifice $\mathcal{H}_\infty$ optimality by minimizing $\alpha_\varepsilon(\cdot)$ for fixed ε. That is,

$$\begin{aligned} \mathbf{A}_\varepsilon: \quad & \underset{x,z,u}{\text{minimize}} \quad \alpha_\varepsilon(A(x, z, u, v)) \\ & \text{subject to} \quad (4) \end{aligned} \tag{12}$$

When $\varepsilon = 0$, $\mathbf{A}_\varepsilon$ finds the optimal configuration u^* that has the fastest asymptotic rate. On the other hand, when $\varepsilon \to +\infty$ the solution of the problem provides a u^* that optimizes the *initial decay rate* of a small perturbation [25].

This new formulation also unveils a fundamental tradeoff between voltage stability and small signal stability of power networks that has not been previously analyzed. Finding the maximum distance to voltage collapse implies using $\alpha_0(A)$ in $\mathbf{A}_\varepsilon$. While the solution of this problem will be optimal in terms of voltage stability margin, it can potentially have transients with large amplitude [18]. On the other hand, if one is interested in minimizing the $\mathcal{H}_\infty(A)$ using $\mathbf{H}_\infty$, then the required voltage stability margins might not be met. This is illustrated in Section IV-A and discussed in Section IV-C.

The optimization problems $\mathbf{H}_\infty$ and $\mathbf{A}_\varepsilon$ conform a novel framework that can be readily combined with the **OPF**. They provide a unifying representation of several dynamical properties within a one parameter family of functions $\alpha_\varepsilon(\cdot)$. This is very convenient as the operator can choose different values of ε, depending on the different needs of the power network in consideration.

This results in the following formulation for a Dynamics-aware Optimal Power Flow problem.

$$\begin{aligned} \textbf{Dyn-OPF}: \quad & \underset{\varepsilon\geq 0,x,z,u}{\text{minimize}} \quad c(V, P_G, Q_G) && (13) \\ & \text{subject to} \quad (4) \\ & \qquad h(\varepsilon) \leq h^* && (14) \\ & \qquad \alpha_\varepsilon(A) = 0 && (15) \\ & \qquad \alpha_{\hat{\varepsilon}}(A) \leq a^* && (16) \end{aligned}$$

where $\hat{\varepsilon}$ is a constant parameter.

The solution to **Dyn-OPF** will provide an operating point that minimizes the generation cost and keeps a maximum power gain of $20\log_{10}(\mathcal{H}_\infty(A)) \leq h^*$. On the other hand, it is possible to use (16) to provide additional constraints on the system. For example, by setting $\hat{\varepsilon} = 0$, (16) can be used to impose specific voltage stability margins. Notice that since neither the **OPF** nor $\mathbf{H}_\infty$ and $\mathbf{A}_\varepsilon$ are convex problems, all their solutions and the solution to **Dyn-OPF** are local minima.

IV. Test Cases

In this section we provide two examples to illustrate the properties of the optimization framework presented in Section III. The dynamic models of (6) and (10) as well as the algebraic equations (4a) and (7) are computed using the *Power System Toolbox* (PST) [26]. $\alpha_\varepsilon(A)$ is evaluated using the Matlab code provided with [27] with a tolerance of $1e{-}12$. The gradients of $\alpha_\varepsilon(A)$ are computed numerically and the Matlab Optimization Toolbox is used to compute the local optimum. We call the *fmincon* subroutine with function and constraint tolerance of $1e{-}6$ for optimizations involving $\alpha_\varepsilon(A)$ ($\mathbf{H}_\infty$, **Dyn-OPF** , $\mathbf{A}_\varepsilon$) and with tolerance $1e-7$ for **OPF** . All the results presented in this section are in base 100MVA.

The cost function $c(V, P_G, Q_G)$ used is the standard quadratic cost function depending only on the active generation, i.e.

$$c(P_G) = \sum_{k\in\mathcal{N}} c_{2k}P_{G_k}^2 + c_{1k}P_{G_k} + c_{0k}.$$

This framework is not limited to this specific $c(V, P_G, Q_G)$ and can be easily extended to consider other objective functions.

A. Two Area Test Case

This example illustrates properties and differences between the local minima of the optimization problems $\mathbf{H}_\infty$, $\mathbf{A}_\varepsilon$ and **OPF**. We consider a 2 area power network with 13 buses and 4 generators with detailed 2-axis subtransient generators, static exciters, power system stabilizers and 2 induction motors on the load buses 4 and 14.

The load profile as well as the parameters of the induction motors were take from the file `d2asbegp.m` that comes with the PST distribution. The generator dynamics parameters are chosen homogeneously and listed in Table I.

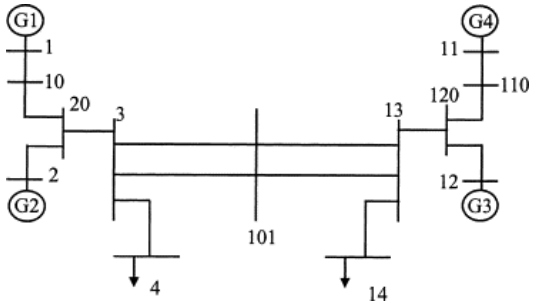

Fig. 1: Two area 13-bus test case

Generators are provided with identical AC4a excitation systems and PSSs. Figure 2 shows a block diagram of the AC4a system, where T_r is the transducer time constant, K_a and T_a are the voltage regulator gain and time constants,

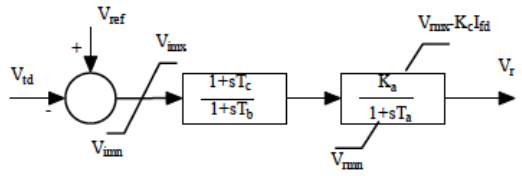

Fig. 2: AC4a Excitation System

respectively, $[V_{i_{\min}}, V_{i_{\max}}]$ are the input voltage saturation limits, $[V_{r_{\min}}, V_{r_{\max}}]$ are the output voltage saturation limits (we take $K_c = 0$ in Figure 2) and T_b and T_c are compensator constants.

We use standard PSSs with washout filter and two lag compensators with Laplace Transfer

$$H_k^{PSS}(s) = \kappa_k \frac{sT_{w,k}}{1+sT_{w,k}} \frac{1+sT_{n1,k}}{1+sT_{d1,k}} \frac{1+sT_{n2,k}}{1+sT_{d2,k}}$$

with equal parameters $\kappa = 1$, $T_w = 10$, $T_{n1} = .05$, $T_{d1} = .02$, $T_{n2} = .08$ and $T_{d2} = .015$. All time constants are in seconds.

We solve **OPF**, $\mathbf{H}_\infty$ and $\mathbf{A}_\varepsilon$ with $\varepsilon = 0$. We assume equal cost among the four generators with parameters $c_0 = 0$ and $c_1 = c_2 = 1$. The optimal power scheduling is illustrated in Table III. Table IV shows the asymptotic rate of convergence $\alpha_0(A)$, minimum damping ratio ξ and maximum gain of the system $\mathcal{H}_\infty(A)$ for the three optimization problems studied in this test case, and Figure 3 shows the corresponding critical eigenvalues.

Table IV also illustrates the tradeoff between asymptotic rate of convergence and transient amplitude. If one tries to maximize the voltage stability margin ($\mathbf{A}_{\varepsilon=\mathbf{0}}$), he obtains a poor damping ratio and high frequency gain $\mathcal{H}_\infty(A)$. However, if one choose to reduce oscillations ($\mathbf{H}_\infty$), the voltage stability margin increases. This confirms our claim suggesting that $\alpha_0(A)$ should not be used as a performance metric in order to avoid oscillations like in [23] as it can potentially amplify them. This is somehow counterintuitive since $\alpha_0(A)$ does succeed in avoiding Hopf Bifurcations.

Additionally, $\mathbf{H}_\infty$ clearly outperforms **OPF** in damping the modes achieving a relative increment in the minimum damping ratio of $\frac{\xi_{\mathbf{H}_\infty}}{\xi_{\mathbf{OPF}}} = 2.83$, almost three times higher, and a gain reduction $\frac{\mathcal{H}_{\mathbf{H}_\infty}(A)}{\mathcal{H}_{\mathbf{OPF}}(A)} = -2.37$ dB. Thus, this example also shows how the dynamic behavior of a power network can be considerably improved by solely changing the operating point. Figure 4 a stem graph of the system modes (damping ratio vs frequency) for the different operating points computed.

B. New England Power Grid

We now consider the IEEE 39-bus New England power grid with 10 detailed 2-axis generator models shown in Figure 5. Generators 1 to 9 are equipped with AC4a excitation system with parameters described also by Table II and PSSs using the optimal configuration described in [6]. The dynamic data of the generators was obtained from [28].

TABLE I: Generator dynamics parameters for the two area test case

Gen #	$\mathbf{x_l}$ (pu)	$\mathbf{r_a}$ (pu)	$\mathbf{x_d}$ (pu)	$\mathbf{x'_d}$ (pu)
1,2,3,4	0.022	0	0.2	0.033
$\mathbf{x''_d(pu)}$	$\mathbf{T'_{do}(sec)}$	$\mathbf{T''_{do}}$ (sec)	$\mathbf{x_q}$ (pu)	$\mathbf{x'_q}$ (pu)
0.028	8	0.03	0.189	0.061
$\mathbf{x''_q}$ (pu)	$\mathbf{T'_{qo}}$ (sec)	$\mathbf{T''_{qo}}$ (sec)	$\mathbf{H}$ (sec)	$\mathbf{d_o = d_1}$ (pu)
0.027	0.4	0.05	58.5	0

TABLE II: AC4a excitation system parameters

Gen #	$\mathbf{T_r}$ (sec)	$\mathbf{K_a}$	$\mathbf{T_a}$ (sec)	$\mathbf{T_b}$ (sec)
1,2,3,4	.0145	200	.05	0
$\mathbf{T_c}$ (sec)	$\mathbf{V_{i_{min}}}$ (pu)	$\mathbf{V_{i_{max}}}$ (pu)	$\mathbf{V_{r_{min}}}$ (pu)	$\mathbf{V_{r_{max}}}$ (pu)
0	-10	10	-4.53	5.64

TABLE III: Power Scheduling of two area 13-bus test case for $\mathbf{H}_\infty$, **OPF** and $\mathbf{A}_\varepsilon$ with $\varepsilon = 0$

Gen #	$\mathbf{H}_\infty$		**OPF**		$\mathbf{A}_\varepsilon$	
	P_G	Q_G	P_G	Q_G	P_G	Q_G
1	6.64	1.04	4.90	0.86	5.86	2.33
2	7.81	2.12	5.01	0.02	5.69	1.65
3	3.59	-1.66	4.89	0.87	5.32	0.72
4	2.00	1.23	5.01	-1.13	3.11	1.51

TABLE IV: Dynamic performance metrics of different operating solutions

	$\mathbf{H}_\infty$	**OPF**	$\mathbf{A}_{\varepsilon=0}$
$\alpha_0(A)$	-0.100238	-0.100331	-0.100598
$\xi(A)$	0.1076	0.0571	0.0108
$\mathcal{H}_\infty(A)$ (dB)	38.23	40.60	55.75

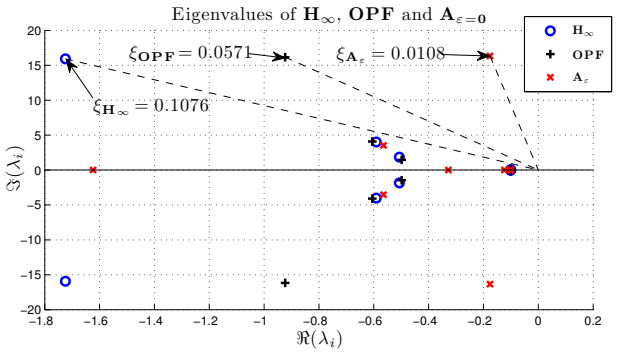

Fig. 3: Eigenvalues of the two area test system in Firgure 1 for the output of **OPF**, $\mathbf{A}_\varepsilon$ with $\varepsilon = 0$ and $\mathbf{H}_\infty$. The counter-clockwise angle between the dashed lines and the horizontal axis θ defines the damping ratio ($\xi = \cos(\theta)$) . Only the eigenvalues closer to the imaginary axis are shown.

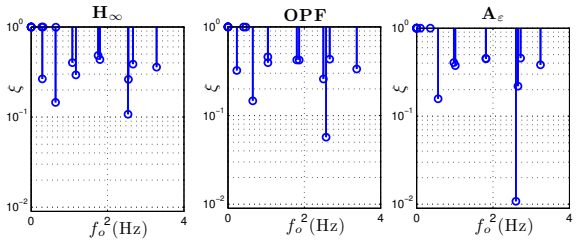

Fig. 4: Modes vs frequency of the two area test system solutions to $\mathbf{A}_\varepsilon$, **OPF** and $\mathbf{H}_\infty$.

We select generator 10 as infinite bus in order to eliminate the zero eigenvalue of the system.

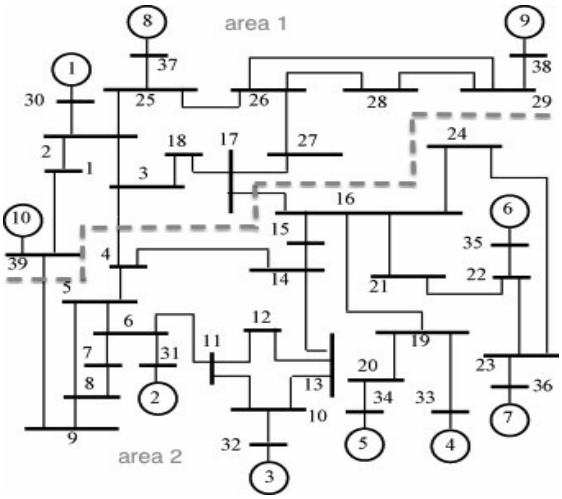

Fig. 5: One line diagram of New England 39-bus system

In order to illustrate a stressed state of the network, we define two different generation cost values. Generators 1, 8-10 use parameters $c_2 = 0.01$, $c_1 = 3.0$ and $c_0 = 0.0$, and generators 2-7 use $c_2 = 0.01$, $c_1 = 0.3$ and $c_0 = 0.0$. This creates a power transfer from area 2 to area 1 of Figure 5 through lines (15.17), $(3, 4)$ and $(9, 39)$ and thus brings the system closer to its stability boundary.

TABLE V: Power Scheduling of **OPF** , $\mathbf{H}_\infty$ and **Dyn-OPF** with $h^* = 32.398$ and $a^* = 0$

Gen #	**OPF**		$\mathbf{H}_\infty$		**Dyn-OPF**	
	P_G	Q_G	P_G	Q_G	P_G	Q_G
1	0.00	1.64	1.97	2.19	10.75	1.84
2	7.75	4.77	10.93	5.01	10.98	4.93
3	7.53	6.78	4.64	5.75	5.47	5.72
4	9.55	5.26	2.40	3.37	2.00	3.38
5	9.09	3.48	10.98	3.16	10.99	3.12
6	10.53	5.33	0.18	2.32	1.34	2.64
7	7.73	2.42	0.71	0.45	8.92	1.63
8	0.00	1.82	11.00	1.56	0.94	1.82
9	0.66	1.09	8.61	0.75	0.01	0.76
10	9.95	2.89	11.00	2.72	11.00	2.29

We first solve the **OPF** and $\mathbf{H}_\infty$ problems with voltage constraints limits of $[0.9, 1.1]$ (pu) for every load bus and $[0.95, 1.05]$ (pu) for every generator bus. Generation limits are set homogeneously to $P_{G_k}^{\max} = 11$, $P_{G_k}^{\min} = 0$, $Q_{G_k}^{\max} = 8$ and $Q_{G_k}^{\min} = -5$. All flow and thermal constraints are made non-binding. The solution of $\mathbf{H}_\infty$ gives a value of $h(\varepsilon^*) = 32.392$ dB while for the optimum of **OPF** $h(\varepsilon^*) = 32.808$ dB. The relative damping ratio gain is $\frac{\xi_{\mathbf{H}_\infty}}{\xi_{\mathbf{OPF}}} = 2.71$ which indicates a significant increment on the system damping.

However, this damping improvement implies an increase of the generation cost from $c(P_G^*) = 59.4$ in **OPF** to $c(P_G^*) = 112.5$ which amounts to a 112.0% increment. This is quite inefficient and we would like to balance the tradeoff between economic efficiency and dynamics performance. We therefore run our **Dyn-OPF** using $h^* = 32.398 \in [32.392, 32.808]$ dB and $a^* = 0$.

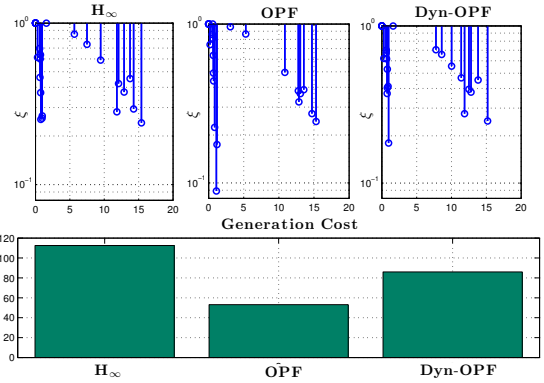

Fig. 6: Damping ratios and generation cost of New England power grid

Figure 6 shows the modes stem graphs for the three different optimization problems solved as well as the generation cost incurred by each. We can see that by allowing a generation cost of $c(P_G^*) = 86.0$, i.e. a 61.9% increment, we are able to obtain a damping ratio gain of $\frac{\xi_{\mathbf{Dyn\text{-}OPF}}}{\xi_{\mathbf{OPF}}} = 2.02$. The corresponding eigenvalues are shown in Figure 7. Although this cost increment might be unfeasible for regular operation, it can certainly be afforded in order to momentarily avoid an unexpected stressed condition.

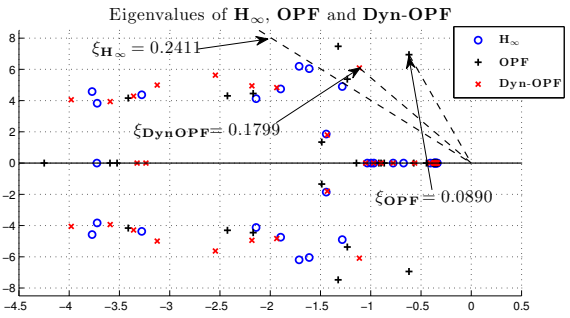

Fig. 7: Critical eigenvalues of New England power grid. The counter-clockwise angle between the dashed lines and the horizontal axis θ defines the damping ratio ($\xi = \cos(\theta)$)

The frequency that maximizes $\mathcal{H}_\infty(A)$ is $\omega = 0$. A detailed analysis of the left and right singular vectors of the singular value $\sigma_{\min}(A) = \sigma_{\max}(j0I - A)^{-1} = \mathcal{H}_\infty(A)$ for the solutions of $\mathbf{H}_\infty$ and **OPF** shows that the high gain of the system transfer function $H(s) = (sI - A)^{-1}$ is achieved between PSS state variables of several groups of generators. This suggests that the system configuration is in a point that is mostly sensitive to changes on the PSSs parameters. It also explains the differences between the power schedulings on Table V and the little gain reduction of -0.41 dB from **OPF** to $\mathbf{H}_\infty$, i.e. one needs considerable changes on the scheduling in order to slightly improve $\mathcal{H}_\infty(A)$.

C. Discussion

There are several outcomes on this section that deserve further discussion. For instance, the tradeoff between voltage

stability margin and transient amplitude may not seem to be a significant problem for this application as utilities are only interested in minimizing the generation cost while guaranteeing fixed stability margins. However, this tradeoff appears in the definition of the margin values themselves. Fixing for instance a large voltage stability margin can hinder the transient behavior of the system.

Additionally, Figures 4 and 6 suggest that some modes are not sensitive to the power scheduling. This evidences some limits of the framework. That is, if the critical modes are not very sensitive to the power scheduling, then the improvement may not be considerable. Therefore, while using stability constraints in the OPF is effective in avoiding stressed scenarios caused by a poor scheduling, it is certainly not a substitute to current industry practices of controller designs which are clearly needed to modify the modes that are not sensitive to the scheduling.

Last but not least, this framework makes evident the fact that as the operating point of the network changes, the optimal parameters that may have been obtained in the controller design stage, as in [6] for PSSs, is no longer optimal.

V. Conclusions and Future Work

This paper present a new optimization framework that aims to close the gap between the market based power dispatch and the security analysis that enforces predefined stability margins and generates re-dispatching. Unlike previous works that consider constraints on the region of the eigenvalues to either guarantee voltage stability or reduce small signal oscillations, we propose the use of pseudo-spectral abscissa as a unifying metric that jointly guarantees both. Our framework not only balances the tradeoff between robustness and economic efficiency, but it also allows the characterization of the performance limits of the system. We verify the efficacy of our formulation using two test cases including the widely used IEEE 39-bus New England test case.

As a future work, we are interested in extending our framework to include controller synthesis. Optimal controllers are usually designed based on a fixed base operating point. However, as the state of the grid changes the designed controllers are no longer optimum. In order to cope with the future challenges of the incursion of renewable generation, the future grid must be able to adapt and reconfigure the controlling scheme online. We are also interested in expanding our framework to include additional performance metrics such as $\mathcal{H}_2$ norm.

References

[1] J. Carpentier, "Contribution to the economic dispatch problem," *Bulletin Society Francaise Electriciens*, vol. 3, no. 8, pp. 431–447, 1962.

[2] R. A. Jabr, A. H. Coonick, and B. J. Cory, "A primal-dual interior point method for optimal power flow dispatching," *Power Systems, IEEE Transactions on*, vol. 17, no. 3, pp. 654–662, 2002.

[3] L. Vargas, V. Quintana, and A. Vannelli, "A tutorial description of an interior point method and its applications to security-constrained economic dispatch," *IEEE Transactions on Power Systems*, vol. 8, pp. 1315 –1324, Aug. 1993.

[4] R. Sugarman, *New York City's blackout: a $350 million drain*. 1978.

[5] C. A. Cañizares, "Applications of optimization to voltage collapse analysis," in *IEEE-PES Summer Meeting, San Diego, USA*, 1998.

[6] R. Jabr, B. Pal, N. Martins, and J. Ferraz, "Robust and coordinated tuning of power system stabiliser gains using sequential linear programming," *IET Generation, Transmission Distribution*, vol. 4, pp. 893 –904, Aug. 2010.

[7] A. H. El-Abiad and K. Nagappan, "Transient stability regions of multimachine power systems," *Power Apparatus and Systems, IEEE Transactions on*, no. 2, pp. 169–179, 1966.

[8] G. Ejebe, G. Irisarri, S. Mokhtari, O. Obadina, P. Ristanovic, and J. Tong, "Methods for contingency screening and ranking for voltage stability analysis of power systems," in *Power Industry Computer Application Conference, 1995. Conference Proceedings., 1995 IEEE*, pp. 249–255, IEEE, 1995.

[9] H. D. Chiang, W. Ma, R. J. Thomas, and J. S. Thorp, "A tool for analyzing voltage collapse in electric power systems PSCC," 1990.

[10] B. Chaudhuri, B. Pal, A. Zolotas, I. Jaimoukha, and T. Green, "Mixed-sensitivity approach to h infin; control of power system oscillations employing multiple FACTS devices," *IEEE Transactions on Power Systems*, vol. 18, pp. 1149 – 1156, Aug. 2003.

[11] X. Xiaorong, X. Jinyu, T. Luyuan, and H. Yingduo, "Inter-area damping control of interconnected power systems using wide-area measurements [j]," *Automation of Electric Power Systems*, vol. 2, no. 28, pp. 37–40, 2004.

[12] C. K. Tang, C. E. Graham, M. El-Kady, and R. T. H. Alden, "Transient stability index from conventional time domain simulation," *IEEE Transactions on Power Systems*, vol. 9, pp. 1524–1530, Aug. 1994.

[13] H.-D. Chiang, *Direct Methods for Stability Analysis of Electric Power Systems: Theoretical Foundation, BCU Methodologies, and Applications*. Wiley. com, 2011.

[14] M. Pavella and P. G. Murthy, "Transient stability of power systems: theory and practice," 1994.

[15] R. Zarate-Minano, F. Milano, and A. Conejo, "An OPF methodology to ensure small-signal stability," *IEEE Transactions on Power Systems*, vol. 26, pp. 1050 –1061, Aug. 2011.

[16] W. Rosehart, C. Cañizares, and V. Quintana, "Optimal power flow incorporating voltage collapse constraints," in *Power Engineering Society Summer Meeting, 1999. IEEE*, vol. 2, pp. 820–825, 1999.

[17] A. Conejo, F. Milano, and R. Garcia-Bertrand, "Congestion management ensuring voltage stability," in *2008 IEEE Power and Energy Society General Meeting - Conversion and Delivery of Electrical Energy in the 21st Century*, pp. 1 –8, July 2008.

[18] J. V. Burke, A. S. Lewis, and M. L. Overton, "Two numerical methods for optimizing matrix stability," *Linear Algebra and its Applications*, vol. 351–352, pp. 117–145, Aug. 2002.

[19] A. Santos Jr and G. R. M. Da Costa, "Optimal-power-flow solution by newton's method applied to an augmented lagrangian function," in *Generation, Transmission and Distribution, IEE Proceedings-*, vol. 142, pp. 33–36, 1995.

[20] I. Dobson and L. Lu, "New methods for computing a closest saddle node bifurcation and worst case load power margin for voltage collapse," *Power Systems, IEEE Transactions on*, vol. 8, no. 3, pp. 905–913, 1993.

[21] C. A. Canizares, A. Berizzi, and P. Marannino, "Using FACTS controllers to maximize available transfer capability," *Proc. Bulk Power Systems Dynamics and Control IV-Restructuring*, pp. 633–641, 1998.

[22] C.-C. Chu, *Transient dynamics of electric power systems: Direct stability assessment and chaotic motions*. Ph.D., Cornell University, United States – New York, 1996.

[23] J. Condren and T. Gedra, "Expected-security-cost optimal power flow with small-signal stability constraints," *IEEE Transactions on Power Systems*, vol. 21, pp. 1736 –1743, Nov. 2006.

[24] K. Zhou, J. C. Doyle, and K. Glover, *Robust and optimal control*, vol. 40. Prentice Hall Upper Saddle River, NJ, 1996.

[25] J. V. Burke, A. S. Lewis, and M. L. Overton, "Optimization and pseudospectra, with applications to robust stability," *SIAM Journal on Matrix Analysis and Applications*, vol. 25, no. 1, pp. 80–104, 2003.

[26] J. H. Chow and K. W. Cheung, "A toolbox for power system dynamics and control engineering education and research," *Power Systems, IEEE Transactions on*, vol. 7, no. 4, pp. 1559–1564, 1992.

[27] D. Kressner and B. Vandereycken, "Subspace methods for computing the pseudospectral abscissa and the stability radius," 2012.

[28] M. A. Pai, *Energy function analysis for power system stability*. Springer, 1989.